

**QED contribution to the production of  $J/\psi + c\bar{c} + X$  at the Tevatron and LHC**

Zhi-Guo He, Rong Li, and Jian-Xiong Wang

*Institute of High Energy Physics, Chinese Academy of Science, P.O. Box 918(4), Beijing, 100049, China and Theoretical Physics**Center for Science Facilities, CAS, Beijing, 100049, China*

(Received 14 April 2009; published 7 May 2009)

We calculate  $\alpha^2\alpha_s^2$  order QED contribution to  $J/\psi$  production in the  $pp(\bar{p}) \rightarrow J/\psi + c\bar{c}$  color-singlet process at the Tevatron and LHC in the framework of nonrelativistic QCD. The contribution of the interference between the  $\alpha^2\alpha_s^2$  QED and  $\alpha_s^4$  QCD is also taken into account. The  $J/\psi$  production associated with a charm-quark pair could be a measurable signal at hadron collider experiment. Our calculations show that by including the QED contribution, the  $p_t$  distribution is enhanced by a factor of 1.5 (1.9) at the Tevatron (LHC) at  $p_t = 50(100)$  GeV. In addition, the polarization of  $J/\psi$  turns from unpolarized in all regions to increasingly transverse when  $p_t$  becomes larger.

DOI: 10.1103/PhysRevD.79.094003

PACS numbers: 12.38.Bx, 13.85.Ni, 14.40.Gx

**I. INTRODUCTION**

Heavy-quarkonium production provides important tests on our understanding of QCD in both perturbative and nonperturbative aspects. Since the heavy quark mass is larger than  $\Lambda_{\text{QCD}}$ , heavy quarkonia are commonly thought to be nonrelativistic bound states. Now the nonrelativistic QCD (NRQCD) effective theory [1] is widely accepted to study the heavy-quarkonium phenomenology (for a review see [2]). In the framework of NRQCD, the production rates of heavy quarkonium could be calculated with a rigorous factorization formula based on the double expansions of the QCD coupling constant  $\alpha_s$  and heavy quark relative velocity  $v$  in the heavy mesons.

The vital difference between NRQCD and traditional color-singlet model is that the NRQCD allows the production of heavy quark pair in color-octet configuration over short distance, and the color-octet state consequently evolves into the physical heavy quarkonium through the nonperturbative emission of soft gluons. The introduction of the color-octet mechanism [3] has successfully reconciled the orders of magnitude discrepancies between the experimental data measured by the CDF Collaboration [4] and the color-singlet model theoretical predictions [5]. However, the CDF former [6] and latest [7] measurements of  $J/\psi$  being almost unpolarized conflict with the NRQCD transverse polarization predictions [8]. So the  $J/\psi$  production mechanism is still a big challenge, and various theoretical attempts can be found in Refs. [9–11].

Recently, substantial progress has been achieved in the calculation of high order QCD corrections to  $J/\psi$  hadroproduction, which are very helpful to clarify the big puzzle. The next-to-leading-order (NLO) QCD corrections [12] to color-singlet  $gg \rightarrow J/\psi g$  production enhance the leading-order (LO) cross section by a factor of 2. Moreover, the NLO result has a large impact on the transverse momentum ( $p_t$ ) distribution of the production rate. It is because the  $p_t$  distribution of the LO result behaves as  $1/p_t^8$ , while the

NLO result behaves as  $1/p_t^6$  due to involving the new topological Feynman diagrams. It is also found [13,14] that the color-singlet  $J/\psi$  production in association with the  $c\bar{c}$  pair process  $gg \rightarrow J/\psi + c\bar{c}$  also has sizable contribution to the  $\alpha_s^4$  (NLO) corrections. This process is also investigated in the  $k_T$  factorization formula [15]. Furthermore, it is reported [16] that the polarization of  $J/\psi$  production via the color-singlet  $^3S_1$  state turns from more transverse to more longitudinal after including the NLO QCD corrections, and most of the  $J/\psi$  produced via color-octet  $^1S_0$  and  $^3S_1$  states at QCD NLO are still almost in a transverse polarization state [17] in the large  $p_t$  region. Toward the resolution of the puzzle on  $J/\psi$  production mechanism, the study has been extended to looking for other possible experimental observable  $J/\psi$  production processes.  $J/\psi$  production associated with a photon in the process  $pp(\bar{p}) \rightarrow J/\psi + \gamma$  is studied in Ref. [18]. Its NLO correction has recently been performed in Ref. [19] and the real next-to-next-to-leading-order (NNLO) analysis has been obtained in Ref. [20]. Double  $J/\psi$  hadroproduction has been studied in Ref. [21].

Among these attempts, the study on the  $J/\psi$  associated production, i.e.  $J/\psi + c\bar{c} + X$  is very interesting. The reasons come from two sides. Experimentally, the cross section of the associated production could be measured by searching for  $J/\psi$  together with  $D\bar{D}$  pair, where  $D$  denotes all possible charm hadrons such as  $D_0$ ,  $D^+$ ,  $D^*$ ,  $\Lambda_c$ , etc. Theoretically, it is noticed [22] that at NNLO the infrared divergence appears due to the soft interaction between the associated  $c$  or  $\bar{c}$  quark and the  $c\bar{c}$  pair in charmonium. Hence, such processes are nonfactorizable at NNLO. And the color-transfer enhancement is introduced in the double-heavy-quark-pair production process. One persuasive example is the recent measurements in  $e^+e^-$  annihilation at center-of-mass energy  $\sqrt{s} = 10.6$  GeV at  $B$  factories for the inclusive and exclusive charmonium production via double charm-quark pairs. Belle collaboration first found [23]

$$\frac{\sigma(e^+e^- \rightarrow J/\psi + c\bar{c})}{\sigma(e^+e^- \rightarrow J/\psi + X)} = 0.59_{+0.15}^{-0.13} \pm 0.12, \quad (1)$$

which is confirmed by their latest analysis [24]. The experimental result is about 6 times larger than the NRQCD predictions at LO in  $\alpha_s$  and  $v$  [25]. The problem is resolved by the recent NLO QCD corrections to inclusive  $J/\psi$  production at  $B$  factories [26]. Another example is that the associated production process  $J/\psi + c\bar{c}$  is also found to be important in  $J/\psi$  photoproduction [27].

During the procedure of studying the charmonium production in  $e^+e^-$  annihilation, it is found that the QED contribution is sizable since the  $J^{\text{PC}} = 1^{--}$  state  $J/\psi$  can be produced via one photon fragmentation. For example, (a) the cross section is very large in  $J/\psi$  electromagnetic production at  $e^+e^-$  colliders [28]; (b) in  $e^+e^- \rightarrow J/\psi + \eta_c$  process, the contribution of the interference between QCD and QED could enhance that of the QCD result by 20%, although the ratios of the QED contribution to the QCD contribution is about 1% [29]; (c) the production rate of  $e^+e^- \rightarrow J/\psi + J/\psi$  [30] at LO is about 3.7 times larger than that of  $e^+e^- \rightarrow J/\psi + \eta_c$  [29] at  $\sqrt{s} = 10.6$  GeV, although the QCD correction to the former process is negative [31]; (d) when the center-of-mass energy  $\sqrt{s} > 20$  GeV [32], the  $J/\psi + c\bar{c}$  produced in  $e^+e^-$  annihilation through two virtual photons will prevail over that through one virtual photon.

In this situation, it is necessary to examine what will happen in  $J/\psi$  hadroproduction after including the QED contribution. Our previous work [33] has shown that the photon fragmentation process up to QCD NLO is very important for the  $p_t$  distribution of the production and polarization of  $J/\psi$  hadroproduction, though its contribution to the total cross section is negligible compared to the QCD contribution. As mentioned above, the  $J/\psi$  associated production is also a very interesting process. Following our previous work, we study in detail the QED effect on  $J/\psi + c\bar{c}$  hadroproduction at the Tevatron and LHC in this paper. The rest of the paper is organized as follows: In Sec. II, we briefly introduce the basic formulas and input parameters used in our calculation. In Sec. III, we discuss the QED contribution to the  $p_t$  distributions of  $J/\psi$  production and polarizations for the associated  $J/\psi$  hadroproduction at the Tevatron and LHC. The conclusion is presented in Sec. IV.

## II. BASIC FORMULAS

According to the NRQCD factorization approach [1], the  $J/\psi + c\bar{c}$  production rate in hadron-hadron collisions could be expressed as

$$\begin{aligned} \sigma[pp \rightarrow J/\psi + c + \bar{c} + X] &= \sum_{i,j,n} \int dx_1 dx_2 G_{i/p} G_{j/p} \\ &\times \hat{\sigma}[i + j \rightarrow (c\bar{c})_n \\ &+ c + \bar{c} + X] \langle \mathcal{O}_n^H \rangle, \quad (2) \end{aligned}$$

where  $p$  is either a proton or antiproton. The short distance part  $\hat{\sigma}$  represents the partonic production of  $c\bar{c}$  with quantum number  $n$ .  $\langle \mathcal{O}_n^H \rangle$  is the nonperturbative long-distance matrix element that parametrizes the transition of the  $c\bar{c}$  pair into  $J/\psi$ .

The QCD contribution to  $pp(\bar{p}) \rightarrow J/\psi + c\bar{c} + X$  starts at  $\alpha_s^4$  order with two independent partonic processes:  $gg \rightarrow c\bar{c} [{}^{2S+1}L_J, \underline{1}(8)] + c + \bar{c}$  and  $q\bar{q} \rightarrow c\bar{c} [{}^{2S+1}L_J, \underline{1}(8)] + c + \bar{c}$ , where  $q$  represents all possible light quarks  $u, d, s$ .  $c\bar{c} [{}^{2S+1}L_J, \underline{1}(8)]$  denotes the specific state of  $c\bar{c}$  with total spin  $S$ , orbital angular momentum  $L$ , total angular momentum  $J$  and 1 (color-singlet) or 8 (color-octet). The contributions of  $J/\psi$  production via the color-singlet  $c\bar{c} [{}^3S_1, \underline{1}]$ , color-octet  $c\bar{c} [{}^3S_1, \underline{8}]$ , and  $c\bar{c} [{}^1S_0, \underline{8}]$  states in the  $gg$  fusion processes have been considered in Refs. [13,14,34]. Since only the  $c\bar{c} [{}^3S_1, \underline{1}]$  state can directly couple with one photon, which may bring kinematic enhancement, in this work, we consider the QED contributions from two processes:

$$\begin{aligned} g(k_1)g(k_2) &\rightarrow c\bar{c} [{}^3S_1, \underline{1}](p_1) + c(p_2) + \bar{c}(p_3), \\ q(k_1)\bar{q}(k_2) &\rightarrow c\bar{c} [{}^3S_1, \underline{1}](p_1) + c(p_2) + \bar{c}(p_3). \quad (3) \end{aligned}$$

The amplitude at parton level is expressed as

$$\begin{aligned} \mathcal{M}[i(k_1)j(k_2) \rightarrow c\bar{c} [{}^3S_1, \underline{1}](p_1) + c(p_2) + \bar{c}(p_3)] \\ = \sum_{s_1, s_2} \sum_{3k, \bar{3}l} \langle s_1; s_2 | 1S_z \rangle \langle 3k; \bar{3}l | 1 \rangle \\ \times \mathcal{M} \left[ i(k_1)j(k_2) \rightarrow c_k \left( \frac{p_1}{2}, s_1 \right) \right. \\ \left. + \bar{c}_l \left( \frac{p_1}{2}, s_2 \right) + c(p_2) + \bar{c}(p_3) \right], \quad (4) \end{aligned}$$

where  $i, j$  are gluon or quarks,  $\langle 3k; \bar{3}l | 1 \rangle = \delta_{kl} / \sqrt{N_c}$  and  $\langle s_1; s_2 | 1S_z \rangle$  are  $SU(3)$ -color and  $SU(2)$ -spin Clebsch-Gordon coefficients for  $c\bar{c}$  pair projecting onto the color-singlet  ${}^3S_1$  state. At LO in  $v$ , the projection operator of Dirac spinor is [35]:

$$\begin{aligned} P_{1, S_z}(p_1) &\equiv \sum_{s_1, s_2} \langle s_1; s_2 | 1S_z \rangle v \left( \frac{p_1}{2}, s_1 \right) \bar{u} \left( \frac{p_1}{2}, s_2 \right) \\ &= \frac{1}{2\sqrt{2}} \not{\epsilon}(S_z) (\not{p}_1 + 2m_c). \quad (5) \end{aligned}$$

To obtain the polarization distribution, the polarization vectors  $\epsilon^\mu(\lambda)$  are kept explicitly during our calculation. The partonic differential cross section for polarized  $J/\psi$  can be written as

$$\frac{d\hat{\sigma}}{dp_t} = A \epsilon(\lambda) \cdot \epsilon^*(\lambda) + \sum_{i,j=1,2} A_{ij} p_i \cdot \epsilon(\lambda) p_j \cdot \epsilon^*(\lambda), \quad (6)$$

where  $\lambda = T_1, T_2, L$ .  $\epsilon(T_1)$ ,  $\epsilon(T_2)$  and  $\epsilon(L)$  are the two transverse polarization vectors and the longitudinal one for  $J/\psi$ , respectively.  $A$  and  $A_{i,j}$  are the coefficients. The polarization parameter  $\alpha$  is defined as

$$\alpha(p_t) = \frac{d\sigma_T/dp_t - 2d\sigma_L/dp_t}{d\sigma_T/dp_t + 2d\sigma_L/dp_t}. \quad (7)$$

We chose physical gauge for gluons to avoid computing the ghost diagrams. The gauge invariance is checked to ensure the validity of our results by replacing the gluon polarization vector with its momentum in numerical computation. Moreover, the long-distance matrix element  $\langle \mathcal{O}_1^{J/\psi} \rangle$  is estimated from the leptonic decay of  $J/\psi$  using the relation

$$\langle \mathcal{O}_1^{J/\psi} \rangle = \frac{2N_c(2J+1)|R_{J/\psi}(0)|^2}{4\pi}. \quad (8)$$

At NLO in  $\alpha_s$  and LO in  $v$ , we have  $\Gamma(J/\psi \rightarrow e^+e^-) = \frac{4\alpha^2}{9m_c^2}(1 - 16\alpha_s/3\pi)|R_{J/\psi}(0)|^2$ . We employ the Feynman Diagram Calculation package [36] to generate the Feynman diagrams and calculate the invariant amplitudes numerically with the basic formulas mentioned above.

The  $pp(\bar{p}) \rightarrow J/\psi + c\bar{c}$  process is part of the QCD real corrections to the  $\alpha_s\alpha^2$  order  $J/\psi$  inclusive production. So we chose the same set of numerical inputs as our last work with

- (i) QCD coupling constant:  $\alpha_s(M_z) = 0.118$ ;
- (ii) renormalization scale  $\mu_r$  and factorization scale  $\mu_f$ :  
 $\mu_r = \mu_f = \mu_0 = \sqrt{(2m_c)^2 + p_t^2}$ ;
- (iii) QED coupling constant:  $\alpha = 1/128$ ;
- (iv) charm-quark mass:  $m_c = 1.5$  GeV;

- (v)  $J/\psi$  leptonic decay width:  $\Gamma(J/\psi \rightarrow e^+e^-) = 5.55$  keV [37];
- (vi) long-distance matrix element  $\langle \mathcal{O}_1^{J/\psi} \rangle = 1.35$  GeV<sup>3</sup> from the leptonic decay width;
- (vii) PDF set: CTEQ6M [38];
- (viii) kinematic cut:  $p_t > 3$  GeV; and  $|y_{J/\psi}| < 0.6$  (Tevatron),  $|y_{J/\psi}| < 3.0$  (LHC).

### III. QED CONTRIBUTION TO $pp(\bar{p}) \rightarrow J/\psi + c\bar{c}$

To investigate the QED effect in  $pp(\bar{p}) \rightarrow J/\psi + c\bar{c}$ , we present the calculation in three parts : QCD, QED, and their interference. The  $\alpha_s^4$  QCD part of  $gg \rightarrow c\bar{c}[^3S_1, \underline{1}] + c + \bar{c}$  includes 42 Feynman diagrams shown in Fig. 1. While there are only 38 Feynman diagrams for the  $\alpha^2\alpha_s^2$  QED part, which are divided into two types and each type forms a gauge invariant subset. The Type I diagrams shown in Fig. 2 can be obtained by replacing the gluon lines between quarks in the QCD diagrams by photon lines. The Type II diagrams shown in Fig. 3 are similar with some of the gluon fragmentation diagrams for color-octet  $c\bar{c}[^3S_1, \underline{8}] + c + \bar{c}$  production when  $\gamma^* \rightarrow c\bar{c}[^3S_1, \underline{1}]$  is changed into  $g^* \rightarrow c\bar{c}[^3S_1, \underline{8}]$ . So the partonic differential cross sections of the two types QED diagrams have the same  $1/p_t^4$  scale behaviors as the QCD ones [34]. Then the contribution of Type I diagrams will be suppressed by  $(\alpha/\alpha_s)^2$  compared to the color-singlet QCD result in both the small and large  $p_t$  region. However, there is a kinematic enhancement in the Type II diagrams. The rea-

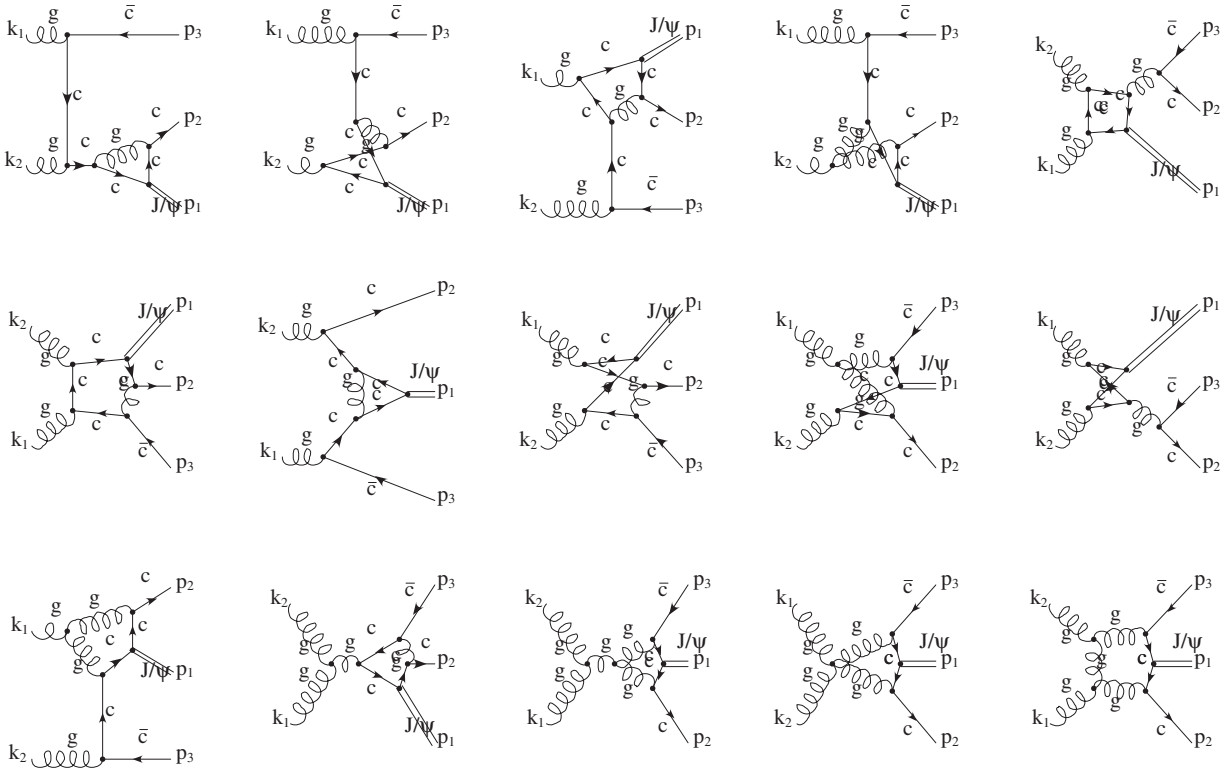


FIG. 1. The typical Feynman diagrams for the  $\alpha_s^4$  QCD part of  $gg \rightarrow c\bar{c}[^3S_1, \underline{1}] + c + \bar{c}$ .

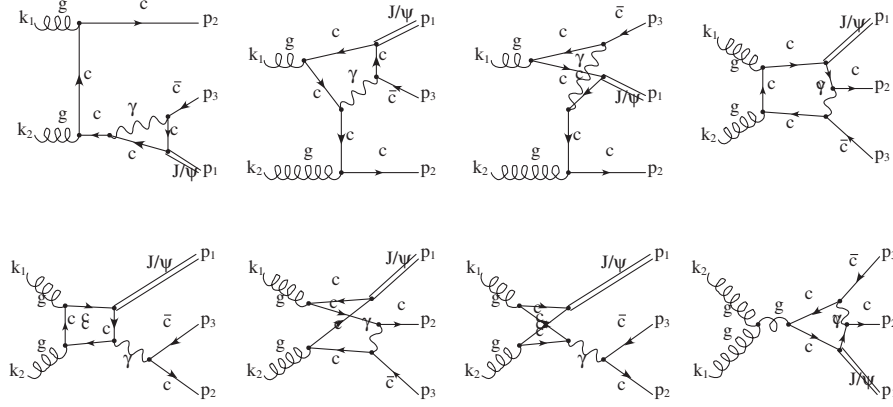


FIG. 2. The typical Type I Feynman diagrams in the LO ( $\alpha^2\alpha_s^2$ ) QED part of  $gg \rightarrow c\bar{c}[{}^3S_1, \underline{1}] + c + \bar{c}$ .

son lies simplify in the fact that the virtuality of the photon in Type II diagrams are fixed to  $4m_c^2$ , whereas it varies from  $4m_c^2$  to  $p_t^2$  order in Type I diagrams. When  $p_t$  is large enough, the kinematic enhancement may compensate the suppression factor  $(\alpha/\alpha_s)^2$ . Furthermore, the value of  $\alpha_s(\mu_0)$  will become smaller as  $p_t$  increasing. We verified that the contribution of Type I diagrams is dominant in small  $p_t$  region and drops fast when  $p_t$  increases. For the  $q\bar{q}$  process, there are 7 QCD and 16 QED Feynman diagrams shown in Fig. 4, and the QED Feynman diagrams also can be divided into two types.

For the QCD contribution alone, we calculate the total cross sections and  $p_t$  distributions of  $J/\psi$  production (dashed lines in Fig. 5(a)) and polarizations (the dashed lines in Fig. 6) for the Tevatron and LHC. The results are in

agreement with the early predictions [13,14,34] when the difference of the parameters are taken into account. And the corresponding total cross sections are

$$\sigma_{\text{QCD}}(p\bar{p} \rightarrow J/\psi + c\bar{c} + X) = 8.7 \text{ nb} \quad (\text{Tevatron}), \quad (9a)$$

$$\sigma_{\text{QCD}}(p\bar{p} \rightarrow J/\psi + c\bar{c} + X) = 169.6 \text{ nb} \quad (\text{LHC}). \quad (9b)$$

For the QED contribution alone, the total cross sections are

$$\sigma_{\text{QED}}(p\bar{p} \rightarrow J/\psi + c\bar{c} + X) = 52.3 \text{ pb} \quad (\text{Tevatron}), \quad (10a)$$

$$\sigma_{\text{QED}}(p\bar{p} \rightarrow J/\psi + c\bar{c} + X) = 1.13 \text{ nb} \quad (\text{LHC}). \quad (10b)$$

Since the integrated cross sections are mostly coming from the contribution in small  $p_t$  region, the total cross sections

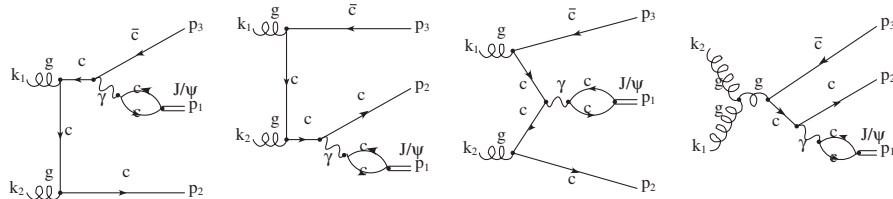


FIG. 3. The typical Type II Feynman diagrams of photon fragmentation in the LO ( $\alpha^2\alpha_s^2$ ) QED part of  $gg \rightarrow c\bar{c}[{}^3S_1, \underline{1}] + c + \bar{c}$ .

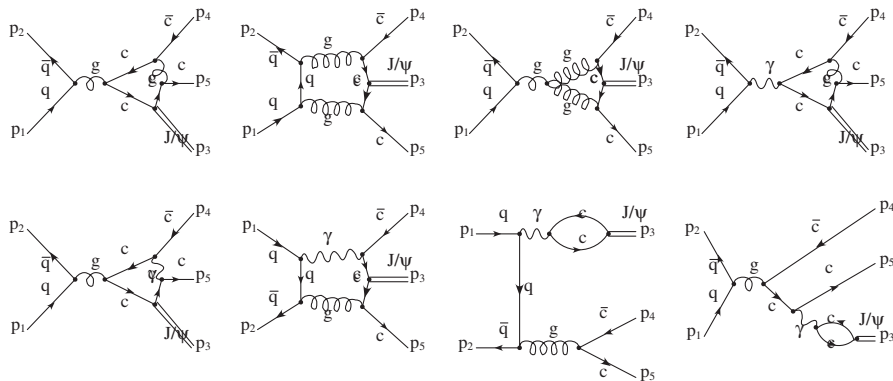


FIG. 4. The typical Feynman diagrams of the LO process of  $q\bar{q} \rightarrow c\bar{c}[{}^3S_1, \underline{1}] + c + \bar{c}$  for QCD and QED.

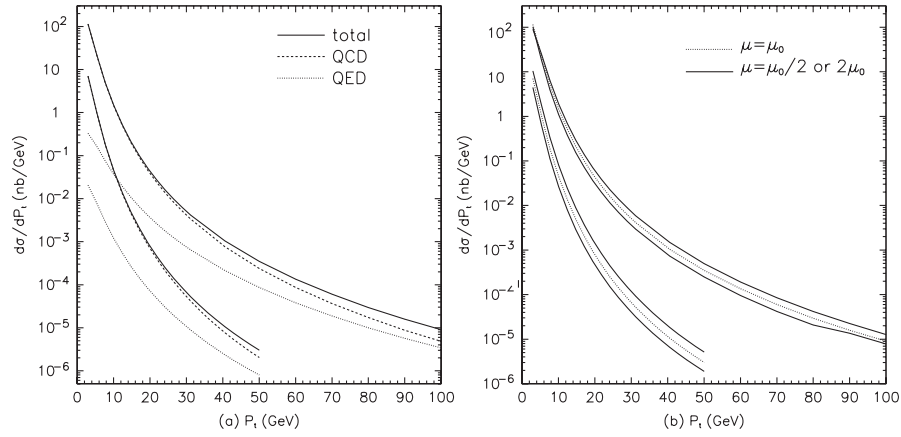


FIG. 5. (a): The  $p_t$  distributions of the production rate for  $J/\psi + c + \bar{c}$  hadroproduction at the Tevatron ( $\sqrt{s} = 1.96$  TeV,  $|y| < 0.6$ ,  $3 \text{ GeV} < p_t < 50 \text{ GeV}$ ) and LHC ( $\sqrt{s} = 14$  TeV,  $|y| < 3$ ,  $3 \text{ GeV} < p_t < 100 \text{ GeV}$ ). (b): the  $p_t$  distributions of the “total” with  $\mu_r = \mu_f = \mu$  dependence. Where the total refers to the sum of the QCD, QED, and their interference results.

of the QED part are about  $(\alpha/\alpha_s)^2 \approx 1/100$  times smaller than the QCD ones for both the Tevatron and LHC.

The  $p_t$  distribution of  $J/\psi$  QED production is shown in Fig. 5 with lower (upper) dotted line for the Tevatron (LHC). It can be seen that the QED contribution is about 2 orders of magnitude less than the QCD contribution at  $p_t = 3 \text{ GeV}$  and the ratio of the QED contribution to the QCD one is 0.4 (0.7) at  $p_t = 50(100) \text{ GeV}$  for the Tevatron (LHC). It means that the QED contribution is indeed negligible in the small  $p_t$  region, but is important in the large  $p_t$  region, especially at the LHC. The  $p_t$  distributions of  $J/\psi$  polarization from the QED part for the Tevatron and LHC are plotted with the dotted-dashed lines in Fig. 6. Both of the curves show that  $J/\psi$  is unpolarized in the small  $p_t$  region and becomes increasingly transverse in the region of large  $p_t$ . It is because the QED part is dominated by the contribution from Type I diagrams in the small  $p_t$  region, while the Type II fragmentation contribution dominates in the large  $p_t$  region.

For the QED part alone, the contribution is comparable to the QCD one in the large  $p_t$  region and particularly the polarization behavior of the former is very different from that of the latter. Therefore, we also calculate the interference between QED and QCD parts. It is found that the interference between the QED and QCD parts of  $pp(\bar{p}) \rightarrow c\bar{c}[^3S_1, \underline{1}] + c\bar{c}$  is positive and the relative phase angle is close to  $\pi/2$ . The total results are shown in Fig. 5(b). The theoretical uncertainties of the  $p_t$  distribution for  $J/\psi$  production are studied by changing the renormalization and factorization scale  $\mu_f = \mu_r$  from  $\mu_0/2$  to  $2\mu_0$ . They correspond to the uncertainty bands of  $J/\psi$   $p_t$  distribution shown in Fig. 5(b). The  $p_t$  distribution of  $J/\psi$  production is enhanced by 50% compared to the QCD result at  $p_t = 50 \text{ GeV}$  at the Tevatron. At the LHC, the enhancement is 190% at  $p_t = 100 \text{ GeV}$ . The  $p_t$  distributions of  $J/\psi$  polarization are shown in Fig. 6. It is shown that the polarization parameter  $\alpha(p_t)$  for the QCD part is almost equals to zero in all regions at both the Tevatron and

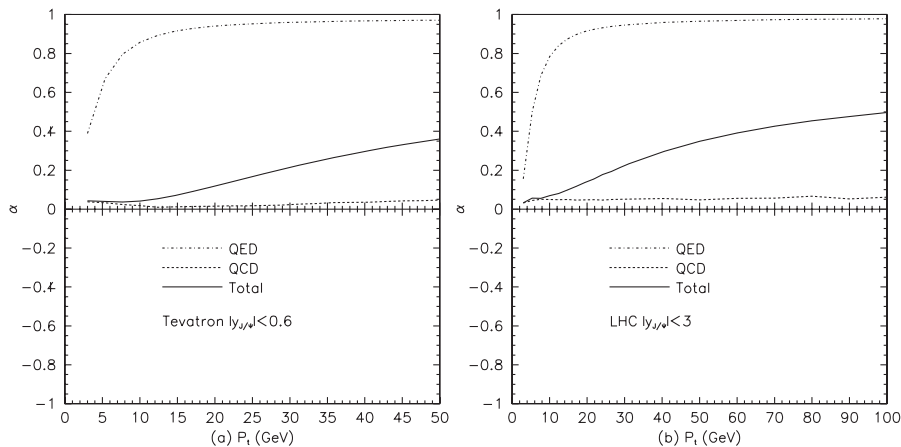


FIG. 6. The  $p_t$  distribution of polarization parameter  $\alpha$  for the  $J/\psi + c + \bar{c}$  hadroproduction at the Tevatron (a) and LHC (b). Here, the total refers to the sum of the QCD, QED and their interference results.



LHC. But it becomes increasing slowly (see the solid line in Fig. 6) when QED part is included in the full calculation.

#### IV. CONCLUSION

Until now, people still have not found a convincing mechanism to explain the  $J/\psi$  hadroproduction at the Tevatron. It is suggested [13] that the associated production channel  $J/\psi + c\bar{c}$ , which may be observed through measurement of the  $J/\psi$  together with at least one charmed hadron, may provide further insight to the mechanism responsible for the  $J/\psi$  hadroproduction. Both the color-singlet and color-octet contributions for the associated  $J/\psi$  production have been calculated at  $\alpha_s^4$  order in Ref. [34]. In this work, we have presented the  $\alpha^2\alpha_s^2$  order calculation for the associated  $J/\psi$  production at the Tevatron and LHC. Our calculation also include the interference terms between the  $\alpha^2\alpha_s^2$  order QED part and  $\alpha_s^4$  QCD color-singlet part. Our results indicate the QED photon fragmentation effect is very important, and it has a large impact on  $p_t$  distribution of  $J/\psi$  production and polarization in large  $p_t$  region, especially for the LHC.

The QED part for  $pp(\bar{p}) \rightarrow J/\psi + c\bar{c}$  is also part of the NLO QCD corrections to photon fragmentation inclusive

$J/\psi$  production considered in our previous work [33]. Both of them scale like  $1/p_t^4$ , so unlike the  $J/\psi$  QCD production case, the impact of the QED  $J/\psi$  associated production contribution on the photon fragmentation inclusive  $J/\psi$  production is not very large for the  $p_t$  distribution of  $J/\psi$  production and polarization.

In this work, we do not study the  $Y$  production associated with the  $b\bar{b}$  pair, though  $Y$  can also be produced by photon fragmentation. There are two reasons. One is the electric charge of bottom-quark is only half of that of charm-quark. It will provide an additional  $(1/2)^4$  suppression factor compared to the charm-quark case. The other is the mass of  $Y$ , which is about 3 times larger than the  $J/\psi$  mass, which makes the photon fragmentation effect for  $Y$  not as outstanding as that for  $J/\psi$  case.

#### ACKNOWLEDGMENTS

This work is supported by the National Natural Science Foundation of China under Contract No. 10775141 and by the Chinese Academy of Science under Project No. KJCX3-SYW-N2.

- 
- [1] G. T. Bodwin, E. Braaten, and G. P. Lepage, Phys. Rev. D **51**, 1125 (1995); **55**, 5853(E) (1997).
  - [2] N. Brambilla *et al.* (Quarkonium Working Group), arXiv: hep-ph/0412158.
  - [3] E. Braaten and S. Fleming, Phys. Rev. Lett. **74**, 3327 (1995).
  - [4] F. Abe *et al.* (CDF Collaboration), Phys. Rev. Lett. **79**, 572 (1997); **79**, 578 (1997).
  - [5] J. H. Kühn, J. Kaplan, and E. G. O. Safiani, Nucl. Phys. **B157**, 125 (1979); C. H. Chang, Nucl. Phys. **B172**, 425 (1980); B. Guberina, J. H. Kühn, R. D. Peccei, and R. Rückl, Nucl. Phys. **B174**, 317 (1980); E. L. Berger and D. Jones, Phys. Rev. D **23**, 1521 (1981); R. Baier and R. Rückl, Z. Phys. C **19**, 251 (1983).
  - [6] A. A. Affolder *et al.* (CDF Collaboration), Phys. Rev. Lett. **85**, 2886 (2000).
  - [7] A. Abulencia *et al.* (CDF Collaboration), Phys. Rev. Lett. **99**, 132001 (2007).
  - [8] M. Beneke and I. Z. Rothstein, Phys. Lett. B **372**, 157 (1996); **389**, 769(E) (1996); M. Beneke and M. Kramer, Phys. Rev. D **55**, R5269 (1997); E. Braaten, B. A. Kniehl, and J. Lee, Phys. Rev. D **62**, 094005 (2000); B. A. Kniehl and J. Lee, Phys. Rev. D **62**, 114027 (2000); A. K. Leibovich, Phys. Rev. D **56**, 4412 (1997).
  - [9] M. Kramer, Prog. Part. Nucl. Phys. **47**, 141 (2001); J. P. Lansberg, Int. J. Mod. Phys. A **21**, 3857 (2006).
  - [10] J. P. Lansberg, arXiv:0811.4005.
  - [11] X. Q. Li, X. Liu, and Z. T. Wei, Front. Phys. China **4**, 49 (2009).
  - [12] J. M. Campbell, F. Maltoni, and F. Tramontano, Phys. Rev. Lett. **98**, 252002 (2007).
  - [13] P. Artoisenet, J. P. Lansberg, and F. Maltoni, Phys. Lett. B **653**, 60 (2007).
  - [14] K. Hagiwara, W. Qi, C. F. Qiao, and J. X. Wang, arXiv:0705.0803.
  - [15] S. P. Baranov, Phys. Rev. D **73**, 074021 (2006); **74**, 074002 (2006).
  - [16] B. Gong and J. X. Wang, Phys. Rev. Lett. **100**, 232001 (2008); Phys. Rev. D **78**, 074011 (2008).
  - [17] B. Gong, X. Q. Li, and J. X. Wang, Phys. Lett. B **673**, 197 (2009).
  - [18] M. Drees and C. S. Kim, Z. Phys. C **53**, 673 (1992); M. A. Doncheski and C. S. Kim, Phys. Rev. D **49**, 4463 (1994); C. S. Kim and E. Mirkes, Phys. Rev. D **51**, 3340 (1995); E. Mirkes and C. S. Kim, Phys. Lett. B **346**, 124 (1995); D. P. ROY and K. Sridhar, Phys. Lett. B **341**, 413 (1995); C. S. Kim, J. Lee, and H. S. Song, Phys. Rev. D **55**, 5429 (1997); P. Mathews, K. Sridhar, and R. Basu, Phys. Rev. D **60**, 014009 (1999); B. A. Kniehl, C. P. Palisoc, and L. Zwirner, Phys. Rev. D **66**, 114002 (2002).
  - [19] R. Li and J. X. Wang, Phys. Lett. B **672**, 51 (2009).
  - [20] J. P. Lansberg, arXiv:0901.4777.
  - [21] V. D. Barger, S. Fleming, and R. J. N. Phillips, Phys. Lett. B **371**, 111 (1996); C. F. Qiao, Phys. Rev. D **66**, 057504 (2002); C. F. Qiao, L. P. Sun, and P. Sun, arXiv:0903.0954; R. Li, Y. J. Zhang, and K. T. Chao, arXiv:0903.2250.
  - [22] G. C. Nayak, J. W. Qiu, and G. Sterman, Phys. Rev. Lett. **99**, 212001 (2007); Phys. Rev. D **77**, 034022 (2008).

- [23] K. Abe *et al.* (Belle Collaboration), Phys. Rev. Lett. **89**, 142001 (2002).
- [24] P. Pakhlov *et al.*, arXiv:0901.2775.
- [25] P.L. Cho and A.K. Leibovich, Phys. Rev. D **54**, 6690 (1996); F. Yuan, C.F. Qiao, and K.T. Chao, Phys. Rev. D **56**, 321 (1997); F. Yuan, C.F. Qiao, and K.T. Chao, Phys. Rev. D **56**, 1663 (1997); S. Baek, P. Ko, J. Lee, and H. S. Song, J. Korean Phys. Soc. **33**, 97 (1998); K. Y. Liu, Z. G. He, and K. T. Chao, Phys. Rev. D **69**, 094027 (2004).
- [26] Y.J. Zhang and K.T. Chao, Phys. Rev. Lett. **98**, 092003 (2007); Y.Q. Ma, Y.J. Zhang, and K.T. Chao, Phys. Rev. Lett. **102**, 162002 (2009); B. Gong and J. X. Wang, Phys. Rev. Lett. **102**, 162003 (2009); arXiv:0904.1103.
- [27] C.F. Qiao and J.X. Wang, Phys. Rev. D **69**, 014015 (2004); P. Artoisenet, F. Maltoni, and T. Stelzer, J. High Energy Phys. 02 (2008) 102; Rong Li and Kuang-Ta Chao, arXiv:0904.1643.
- [28] C.H. Chang, C.F. Qiao, and J.X. Wang, Phys. Rev. D **56**, R1363 (1997); **57**, 4035 (1998).
- [29] E. Braaten and J. Lee, Phys. Rev. D **67**, 054007 (2003); **72**, 099901(E) (2005); K. Y. Liu, Z. G. He, and K. T. Chao, Phys. Rev. D **77**, 014002 (2008).
- [30] G.T. Bodwin, J. Lee, and E. Braaten, Phys. Rev. Lett. **90**, 162001 (2003).
- [31] B. Gong and J.X. Wang, Phys. Rev. Lett. **100**, 181803 (2008).
- [32] K. Y. Liu, Z. G. He, and K. T. Chao, Phys. Rev. D **68**, 031501 (2003).
- [33] Z. G. He, R. Li, and J. X. Wang, arXiv:0904.1477.
- [34] P. Artoisenet, in *The Proceedings of 9th Workshop on Non-Perturbative Quantum Chromodynamics, Paris, France, 2007*, p. 21.
- [35] J.H. Kuhn, J. Kaplan, and E.G.O. Safiani, Nucl. Phys. **B157**, 125 (1979); B. Guberina, J.H. Kuhn, R.D. Peccei, and R. Ruckl, Nucl. Phys. **B174**, 317 (1980).
- [36] J.X. Wang, Nucl. Instrum. Methods Phys. Res., Sect. A **534**, 241 (2004).
- [37] C. Amsler *et al.* (Particle Data Group), Phys. Lett. B **667**, 1 (2008).
- [38] J. Pumplin, D.R. Stump, J. Huston, H.L. Lai, P.M. Nadolsky, and W.K. Tung, J. High Energy Phys. 07 (2002) 012.